



Diurnal hydrochemical variations in a karst spring and two ponds, Maolan Karst Experimental Site, China: Biological pump effects



Huan Liu ^{a,b}, Zaihua Liu ^{c,*}, G.L. Macpherson ^{a,*}, Rui Yang ^c, Bo Chen ^c, Hailong Sun ^c

^a Department of Geology, University of Kansas, 1475 Jayhawk Blvd., 120 Lindley Hall, Lawrence, KS 66045, USA

^b Department of Earth Sciences, The University of Hong Kong, Pokfulam Road, Hong Kong

^c State Key Laboratory of Environmental Geochemistry, Institute of Geochemistry, Chinese Academy of Sciences, 46 Guanshui Road, Guiyang 550002, China

ARTICLE INFO

Article history:

Received 13 September 2014

Received in revised form 3 January 2015

Accepted 3 January 2015

Available online 10 January 2015

This manuscript was handled by Geoff Syme, Editor-in-Chief

Keywords:

Diurnal hydrochemical variation

Surface water system

Biological pump effect

Autochthonous organic matter formation

Carbon sink

SUMMARY

A karst spring and two downstream ponds fed by the spring at the Maolan Karst Experimental Site, Guizhou Province, China, were used to investigate the effect of submerged plants on the CO₂–H₂O–CaCO₃ system during a time of spring base flow in summer when underwater photosynthesis was strongest. Temperature, pH, electrical conductivity (EC) and dissolved oxygen (DO) were recorded at 15 min intervals for a period of 30 h (12:00 29 August–18:00 30 August, 2012). [Ca²⁺], [HCO₃⁻], CO₂ partial pressure (*p*CO₂) and saturation index of calcite (SI_c) were estimated from the high-frequency measurements. Water samples were also collected three times a day (early morning, midday and evening) for δ¹³C_{DIC} determination. A floating CO₂-flux monitoring chamber was used to measure CO₂ flux at the three locations. Results show that there was little or no diurnal variation in the spring water parameters. In the midstream pond with flourishing submerged plants, however, all parameters show distinct diurnal changes: temperature, pH, DO, SI_c, δ¹³C_{DIC} increased during the day and decreased at night, while EC, [HCO₃⁻], [Ca²⁺], and *p*CO₂ behaved in the opposite sense. In addition, maximum DO values (16–23 mg/L) in the midstream pond at daytime were two to three times those of water equilibrated with atmospheric O₂, indicating strong aquatic photosynthesis. The proposed photosynthesis is corroborated by the low calculated *p*CO₂ of 20–200 ppmv, which is much less than atmospheric *p*CO₂. In the downstream pond with fewer submerged plants but larger volume, all parameters displayed similar trends to the midstream pond but with much less change, a pattern that we attribute to the lower biomass/water volume ratio. The diurnal hydrobiogeochemical variations in the two ponds depended essentially on illumination, indicating that photosynthesis and respiration by the submerged plants are the dominant controlling processes. The large loss of DIC between the spring and midstream pond, attributed to biological pump effects, demonstrates that natural surface water systems may constitute an important sink of carbon (on the order of a few hundred tons of C km²/a) as DIC is transformed to autochthonous organic matter. The rates of sedimentary deposition and preservation of this organic matter in the ponds, however, require quantification in future work to fully assess the karst processes-related carbon sink, especially under global climate and land use changes.

© 2015 Elsevier B.V. All rights reserved.

1. Introduction

Hydrochemical behavior in karst terrains exhibits marked annual, seasonal, and even diurnal and storm-scale variations (Liu et al., 2004, 2006, 2007, 2008). Thus, an increasing number of studies have focused on the karst critical zone because of its sensitivity to environmental changes and distinctive

resource–environmental effects (De Montety et al., 2011; Hayashi et al., 2012; Yang et al., 2012; Zeng et al., 2012; Kurz et al., 2013).

Surface waters in karst terrains are rich in dissolved inorganic carbon (DIC) and provide a well-defined natural system to study gas exchange between water and atmosphere, calcite deposition, aquatic photosynthesis and respiration (Spiro and Pentecost, 1991). Previous studies have emphasized particular aspects of geochemistry or biology in these waters, but data on the interactions among physical, chemical and biological processes are still lacking. These mutually dependent processes should be discussed together, because consideration of water–rock–gas–organism interaction as a whole is required to understand the spatiotemporal hydrochemical

* Corresponding authors. Tel.: +86 851 5895263 (Z. Liu), +1 785 8642742 (G.L. Macpherson).

E-mail addresses: liuzaihua@vip.gyig.ac.cn (Z. Liu), glmac@ku.edu (G.L. Macpherson).

variations in karst waters (Liu et al., 2010; Yang et al., 2012). Moreover, due to the dynamics and complexity of karst processes, there is still much to be learned about the biogeochemistry of karst waters, especially diurnal spatiotemporal variation (Liu et al., 2006, 2007, 2008; Yang et al., 2012).

A study of dissolved elemental and carbon isotopic composition in the major karst springs at the Maolan Karst Experimental Site, SW China (Maolan) has provided useful information about the characteristics of spring water. Because different sources of dissolved inorganic carbon (DIC) have different isotopic compositions, $\delta^{13}\text{C}_{\text{DIC}}$ is a direct reflection of the physical, chemical and biological processes in the water (Han et al., 2010). Identifying the transformation of DIC to organic carbon (OC) as evidenced by changes in CO_2 , O_2 , DIC, pH, $\delta^{13}\text{C}_{\text{DIC}}$ and estimating this contribution quantitatively are the purposes of this study.

Here we report on an investigation of an epikarst spring (Liu et al., 2007) and its two downstream ponds at Maolan. We have obtained high time-resolution monitoring records of the physical-chemical parameters for about a 30-hour period (12:00 29 August–18:00 30 August, 2012) when underwater photosynthesis was strongest. We also report selected $\delta^{13}\text{C}_{\text{DIC}}$ from the site. This research focuses on the physical chemistry of karst water and the evolution of $^{13}\text{C}_{\text{DIC}}$ influenced by major natural processes. The aim of this study is to understand diurnal hydrochemical variations and quantitatively estimate the C loss through the biological pump in a typical karst spring and its two downstream ponds under summer, sunny and base flow conditions. These conditions represent the time of most intensive biological activity. The results reveal spatiotemporal differences and their underlying mechanisms, which have implications for assessing karst processes as related to the global carbon sink (Liu et al., 2010).

2. Study area

The Maolan Karst Experimental Site in China (Maolan; Fig. 1) is well known for its dense virgin evergreen forests growing on cone karst, and is listed by UNESCO as a world heritage site (Libo Karst, one of the three clusters of South China Karst, whc.unesco.org). Annual rainfall in areas with virgin forest is about 1750 mm, about 80% of which falls in the monsoon season from April to September, July and August being the months with highest average precipitation (Zhou, 1987). Annual rainfall is 400 mm less in surrounding deforested areas due to absence of the forest microclimatic effect (Zhou, 1987). The mean annual air temperature at Maolan is about 17 °C, with hot summers (June–August) and cold winters (December–February). The bedrock is mostly dolomitic limestone of Middle to Lower Carboniferous age (Liu et al., 2007; Jiang et al., 2008).

The sampled spring is a typical Ca– HCO_3 type epikarst spring (here termed ‘Maolan spring’) with flow rate of 0.05–30 L/s (Liu et al., 2007). It is at the base of a cone karst slope covered by virgin karst forest. There is no net deposition of tufa at the spring and the calcite saturation index of the water there is near zero (Liu et al., 2007). Fig. 2 gives an oblique perspective of the spring and the receiving ponds with different amounts of submerged plants (chiefly *Charophyta*). The spring and two ponds have been modified by the addition of weirs to control outflow. The spring weir was built in 2002 for long-term monitoring of water stage and hydrogeochemistry (Liu et al., 2007), and the weirs for the two ponds were built in 2004 by the local population for freshwater fish farming; fishing was abandoned in 2011.

The spring discharge was 1.2 L/s and almost stable during the study period, and the surface areas of midstream and downstream ponds were 280 m² and 1300 m² respectively. The midstream pond volume was smaller (60 m³) than the downstream pond volume (1300 m³). The distances from the spring orifice sampling site

to the midstream pond sampling site was 38 m, and the distance between the midstream and downstream pond sampling sites was 29 m.

3. Methods

3.1. Field monitoring and sampling

The field study was conducted on 29–30 August 2012 under summer, sunny and base flow conditions, when underwater photosynthesis was strongest. Two WTW[®] (Wissenschaftlich-Technische-Werkstaetten) Technology MultiLine[®] 350i's and one SEBA[®] multi-parameter data logger (Qualilog-16[®]) were programmed to measure pH, water temperature, dissolved oxygen (DO), and electrical conductivity (EC, 25 °C) at 15 min interval for 30 h (12:00 29 August–18:00 30 August, 2012) covering a complete diurnal cycle. The meters were calibrated prior to deployment using pH (4, 7 and 10), EC (1412 $\mu\text{S}/\text{cm}$), and DO (0% and 100%) standards. One WTW-350i[®] was located at the spring orifice to characterize discharging groundwater. The Qualilog-16[®] monitored conditions at the midstream pond and the second WTW-350i[®] monitored the downstream pond. The resolutions on pH, DO, EC and temp are 0.01, 0.01 mg/L, 1 $\mu\text{S}/\text{cm}$ and 0.01 °C, respectively.

Water samples for $\delta^{13}\text{C}_{\text{DIC}}$ were collected three times (midday 29 August; evening 29 August; morning 30 August) at the three sites. The sampling site for the Maolan spring $\delta^{13}\text{C}_{\text{DIC}}$ differed from the location of the multi-parameter meter: the meter was put in the orifice measuring groundwater conditions just before emergence into the spring pool, whereas the $\delta^{13}\text{C}_{\text{DIC}}$ samples were collected in the spring pool, after some equilibration with surface conditions. The $\delta^{13}\text{C}_{\text{DIC}}$ samples were collected in pre-cleaned 30 mL glass vials, with no air space. One drop of saturated HgCl_2 solution was added to each sample to prevent microbial activity and all samples were kept at temperatures below 4 °C until analysis.

A floating CO_2 -flux monitoring chamber (14 L volume with diameter of 40 cm, and surface area of 0.126 m²) was placed on the surface of the waters to determine CO_2 efflux from the three sites. CO_2 flux was evaluated three times (midday 29 August; evening 29 August; morning 30 August) at each location by collecting five floating-chamber gas samples at 2-min intervals. The chamber was emptied between sampling and flushed with ambient air. The CO_2 concentration of the samples was measured by gas chromatography (Agilent-7890[®]) with a resolution of 0.01 ppmv.

3.2. Estimating CO_2 partial pressure and the calcite saturation index

We attribute EC fluctuations in the spring and ponds to Ca^{2+} and HCO_3^- variations induced by calcite precipitation or dissolution because other dissolved components are not involved in dissolution or precipitation reactions, no rainfall occurred during the sampling interval and evaporation is unlikely because of the high humidity (83% annually, www.163gz.com) of Maolan. In karst area with purely a bicarbonate type, Ca^{2+} , Mg^{2+} and HCO_3^- were previously correlated with EC at this site (Liu et al., 2007). The regressions were used to estimate concentrations of Ca^{2+} and HCO_3^- for further calculations, below. The relationships are:

$$[\text{Ca}^{2+}] = 0.15\text{EC} - 0.78, \quad r^2 = 0.94, \quad (1)$$

$$[\text{Mg}^{2+}] = 0.04\text{EC} + 0.22, \quad r^2 = 0.77, \quad (2)$$

$$[\text{HCO}_3^-] = 0.63\text{EC} - 4.70, \quad r^2 = 0.99, \quad (3)$$

where brackets denote concentrations in mg/L and EC is electric conductivity in $\mu\text{S}/\text{cm}$ at 25 °C (Liu et al., 2007).

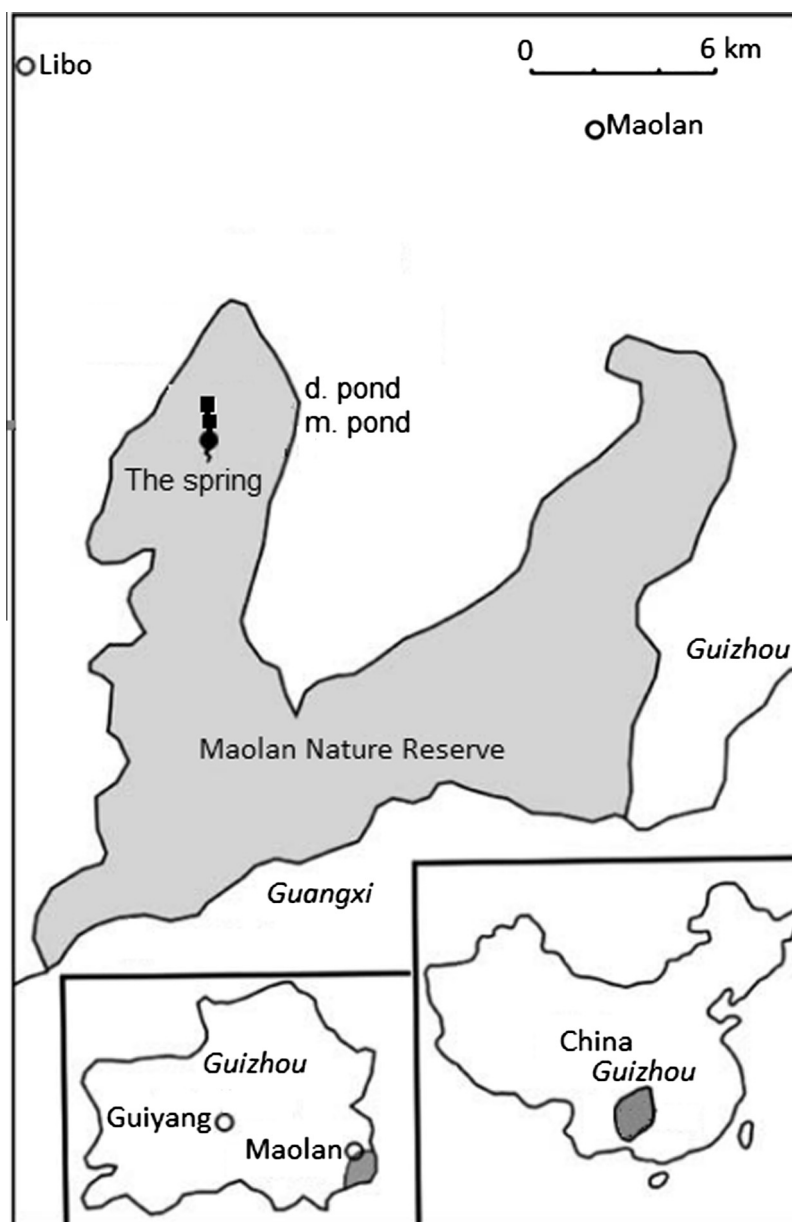


Fig. 1. Location of the Maolan Karst Experimental Site and Maolan spring and the two ponds (monitoring sites) (modified from Jiang et al. (2008)). Due to the short distance between spring and the ponds (<70 m), it is difficult to separate these locations on the map.

Water temperature, pH, derived Ca^{2+} and HCO_3^- , with mean monthly values of K^+ , Na^+ , Mg^{2+} , Cl^- and SO_4^{2-} (resolutions are 0.01 mg/L) (Liu et al., 2007), were speciated using PHREEQC (Parkhurst and Appelo, 1999) to calculate CO_2 partial pressure ($p\text{CO}_2$) and the calcite saturation index (SIc) for each record.

3.3. Determining DIC and $\delta^{13}\text{C}_{\text{DIC}}$

The pH of the water in the study ranged from 7.20 to 9.63. At pH 9.6, HCO_3^- and CO_3^{2-} are 84% and 16% of the DIC, respectively. At pH 9, HCO_3^- and CO_3^{2-} constitute 96% and 4% of the DIC, respectively. However, only four pH points for the midstream pond have values higher than 9.5. Thus, calculated HCO_3^- is used as an approximation of DIC for this study.

$\delta^{13}\text{C}$ was analyzed on a MAT-252 mass spectrometer with dual inlet. The results are reported relative to the V-PDB standard with an uncertainty less than $\pm 0.03\text{‰}$ (Sun et al., 2011).

4. Results

4.1. Diurnal variations in physical chemistry and $\delta^{13}\text{C}_{\text{DIC}}$

Fig. 3 shows the diurnal variations of the physical chemistry of the Maolan spring and ponds during the study of 29–30 August 2012. Each location is discussed separately, below.

(1) Maolan spring

The pH values of the spring water ranged from 7.11 to 7.28, averaging 7.21. Except for fluctuations of DO (coefficient of variation, CV = 4%) and $p\text{CO}_2$ (CV = 6%; Table 1), there was almost no diurnal change in all of the other physical and chemical parameters at the spring (CV < 1.0%, Table 1, Fig. 3). $\delta^{13}\text{C}_{\text{DIC}}$ of Maolan spring was lowest in the sample collected in the morning and highest at midday (Fig. 4).

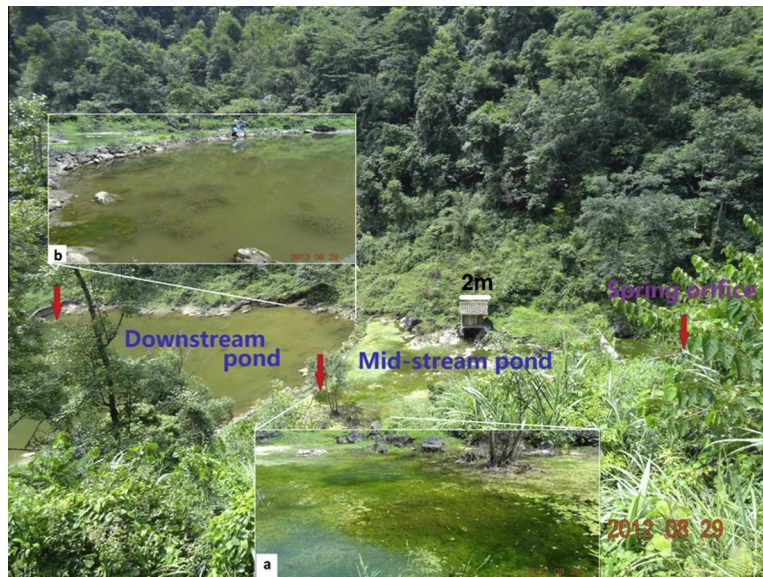


Fig. 2. Maolan spring and the spring-fed midstream pond with flourishing submerged plants (a) and downstream pond with few submerged plants (b) due to use of herbicide by local farmer. The red arrows represent the positions of the measuring points where continuous data were acquired. The surrounding vegetation cover is virgin karst forests.

(2) Midstream pond

All parameters in the midstream pond showed distinct changes over the sampling period (Fig. 3, Table 1). Temperature, pH, DO, Slc and $\delta^{13}\text{C}_{\text{DIC}}$ increased during the day and decreased at night, while EC, HCO_3^- , Ca^{2+} , and $p\text{CO}_2$ decreased in the daytime and increased at night (Figs. 3 and 4).

Water temperature in the midstream pond ranged from 24.2 °C at 8:00 to 31.8 °C at 16:00 in response to insolation; the mean value was 27.7 °C (Fig. 3, Table 1). Correspondingly, pH, DO, Slc and $\delta^{13}\text{C}_{\text{DIC}}$ of the waters increased during the day and peaked at 9.62, 23.49 mg/L, 1.62, and -8.4‰ , respectively, about an hour or two after temperature was the highest. These parameters declined during the night to reach lowest values (7.47, 0.05 mg/L, 0.03, and -12.3‰ , respectively) in the early morning before the sun rose. EC, HCO_3^- , Ca^{2+} and $p\text{CO}_2$ displayed the reverse of this behavior; EC, estimated HCO_3^- , estimated Ca^{2+} and $p\text{CO}_2$ continuously decreasing during the day to a minima (249 $\mu\text{S}/\text{cm}$, 152 mg/L, 37 mg/L, and 20 ppmv, respectively) around 18:00, then gradually increased to a maxima (335 $\mu\text{S}/\text{cm}$, 206 mg/L, 50 mg/L, and 6750 ppmv, respectively) in the early morning.

(3) Downstream pond

All of the parameters in the downstream pond followed patterns similar to those in the midstream pond from morning to midday but at lower amplitude (Fig. 3, Table 1). Water temperature varied from 26.7 °C to 30.5 °C with an average of 28.6 °C, reaching its minimum at about 8:00 and peak at around 16:00. Similarly, EC, estimated HCO_3^- , estimated Ca^{2+} and $p\text{CO}_2$ decreased from 301 $\mu\text{S}/\text{cm}$, 185 mg/L, 44 mg/L and 1430 ppmv respectively at 8:00 to 280 $\mu\text{S}/\text{cm}$, 172 mg/L, 41 mg/L and 660 ppmv at around an hour or two after temperature peaked (Fig. 3, Table 1). pH, DO, and Slc of the water increased from 8.12, 6.95 mg/L, and 0.66 respectively at 8:00 to 8.43, 11.5 mg/L, and 0.93 at about one or two hours after maximum temperature.

4.2. CO_2 flux

(1) Maolan spring

Fig. 5a, Tables 2 and 3 show that CO_2 degassing in the spring pool was the weakest during midday and the most intense in the

evening. In the morning, CO_2 increased from 504 ppmv to 602 ppmv after 8 min, with an efflux of 2500 mg/d/m². During midday, initial CO_2 concentration was 382 ppmv and gradually increased to 416 ppmv after 8 min, with an efflux of 1400 mg/d/m². In the evening, the starting CO_2 concentration in the chamber was 566 ppmv and increased to 660 ppmv over the measurement period of 8 min, with an efflux of 3100 mg/d/m².

(1) Midstream pond

CO_2 concentration ranged from 517 ppmv to 544 ppmv after 6 min and 491 ppmv to 518 ppmv after 8 min in the morning and evening samplings, respectively, (Fig. 5b), with both effluxes of 1100 mg/d/m² (Table 3). During midday, there was no CO_2 outgassing. Instead, atmospheric CO_2 evidently dissolved into the pond water. CO_2 started at 364 ppmv in the chamber then gradually decreased to 273 ppmv after 8 min, with an influx of -3600 mg/d/m².

(3) Downstream pond

CO_2 concentration was the highest in the morning, varying from 534 ppmv to 551 ppmv in the chamber within 8 min, with an efflux of 500 mg/d/m². In the midday and evening, it increased from 385 to 433 ppmv after 8 min and 446 to 470 ppmv after 8 min respectively, with effluxes of 960 mg/d/m² and 560 mg/d/m², correspondingly (Fig. 5c, Table 3).

5. Discussion

5.1. Mechanisms for DIC and $\delta^{13}\text{C}_{\text{DIC}}$ changes in the Maolan spring pool

Atmospheric CO_2 has an isotopic composition of $\delta^{13}\text{C}$ of -7‰ , and the isotopic composition of marine limestone is $0 \pm 5\text{‰}$ (Telmer and Veizer, 1999). Generally speaking, the $\delta^{13}\text{C}$ of CO_2 derived from respiration of C3 plant roots is similar to the $\delta^{13}\text{C}_{\text{CO}_2}$ from degradation of soil organic matter derived from C3 plants, which is close to $-24 \pm 2\text{‰}$ (Cerling et al., 1991; Aucour et al., 1999). According to a recent study in the Maolan spring catchment, $\delta^{13}\text{C}_{\text{DIC}}$ ranges from -8.1‰ to -16.6‰ with a mean value of -13.4‰ (Han et al., 2010), which encompasses the range in this study of -13.4‰ to -14.3‰ , with a mean value of -13.9‰

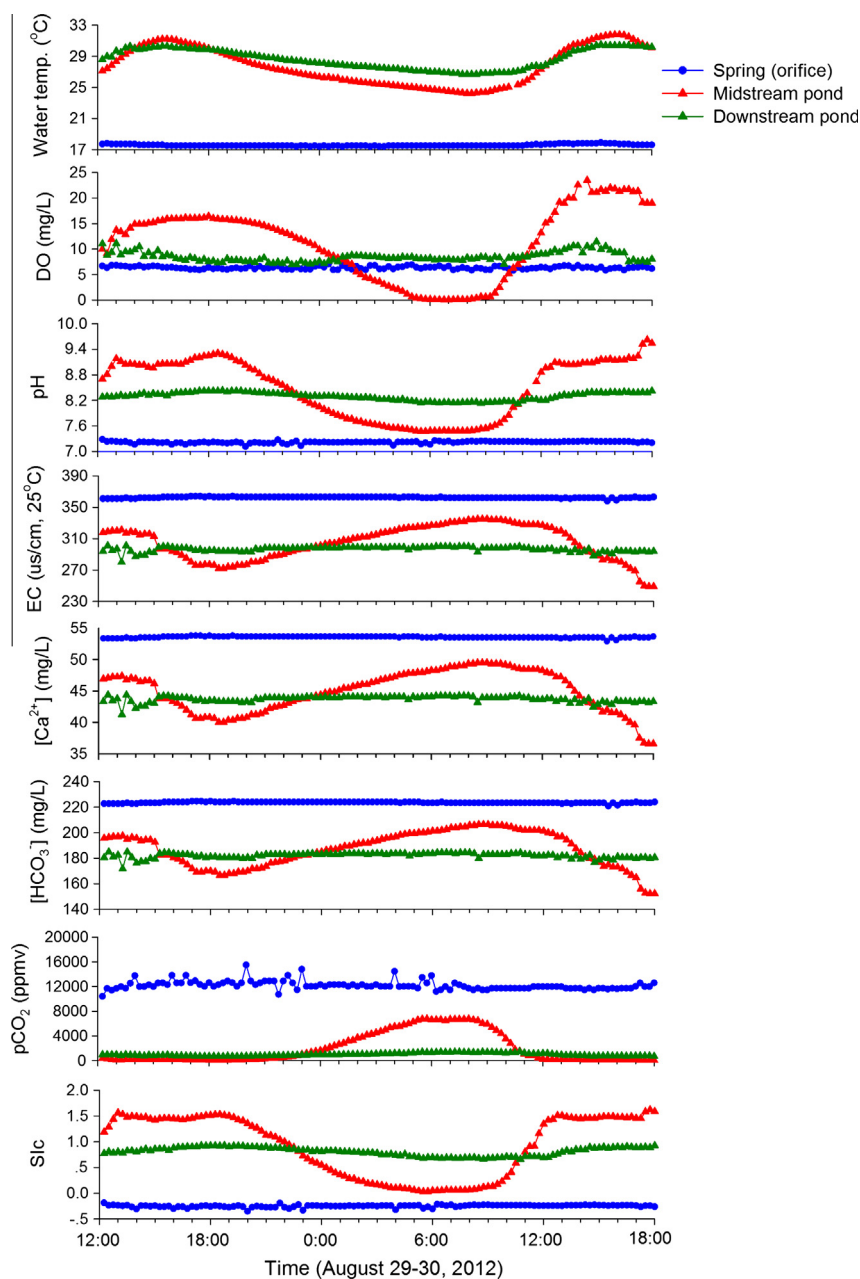


Fig. 3. The diurnal variations of the physical–chemical parameters of Maolan spring (orifice) and the midstream and downstream ponds (2-sigma error bars are smaller than the symbols). Notes: The y axes for $[Ca^{2+}]$, $[HCO_3^-]$, pCO_2 and SI_c are derived values.

Table 1

Daily minimum, maximum, mean values of hydrobiogeochemical parameters in Maolan spring and two ponds during August 29–30, 2012.

Maolan spring					Midstream pond			Downstream pond		
Item	Unit	Min	Max	Mean ($n = 120$)	Min	Max	Mean ($n = 120$)	Min	Max	Mean ($n = 120$)
Temp.	°C	17.4	17.9	17.6	24.2	31.8	27.7	26.7	30.5	28.6
DO	mg/L	5.79	7.05	6.34	0.05	23.49	11.31	6.95	11.46	8.46
pH	–	7.11	7.28	7.21	7.47	9.62	8.5	8.12	8.43	8.29
EC	$\mu s/cm$	358	364	362	249	335	304	280	301	296
Ca^{2+}	mg/L	52.9	53.8	53.6	36.6	49.5	44.8	41.2	44.4	43.7
HCO_3^-	mg/L	220.8	224.6	223.6	152.2	206.4	186.6	172	185	182
SI_c	–	–0.35	–0.19	–0.25	0.03	1.62	0.93	0.66	0.93	0.81
pCO_2	ppmv	10,400	15,500	12,200	20	6750	1910	660	1430	950

(Fig. 4). These $\delta^{13}C$ values are lower than those of karst groundwater measured in city springs in southwest China (Han et al., 2010), the difference attributed to the dense virgin forests in Maolan. Han

et al. (2010) also determined that $56 \pm 9\%$ of the DIC in the Maolan spring water is from degradation of organic matter in the soil and the remainder from dissolution of carbonate.

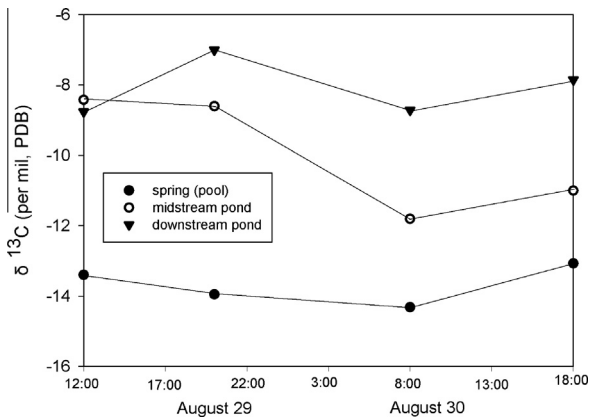


Fig. 4. Diurnal variations in $\delta^{13}\text{C}_{\text{DIC}}$ of the spring pool, midstream pond and downstream pond (2-sigma error bars are smaller than the symbols).

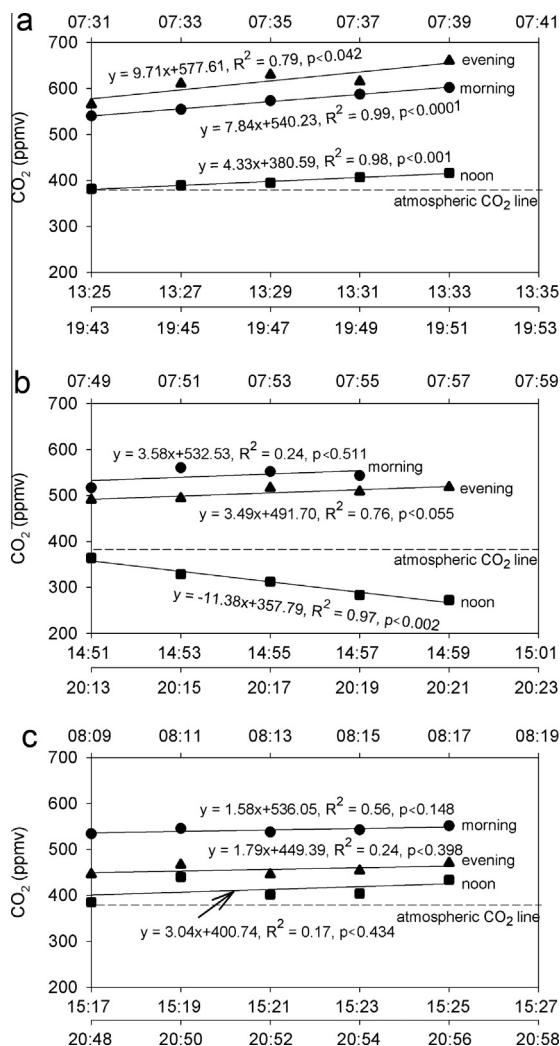


Fig. 5. CO_2 variations in the floating chamber located in the spring pool (a), midstream pond (b) and downstream pond (c) in the early morning, at midday and in the evening (2-sigma error bars are smaller than the symbols).

In this study, the $\delta^{13}\text{C}_{\text{DIC}}$ of the Maolan spring pool started at -13.4‰ at 13:30 on 29 August then decreased to -14.0‰ at 19:40, and continued decreasing to -14.3‰ at 7:30 of 30 August. It is unlikely that the diurnal variation of the $\delta^{13}\text{C}_{\text{DIC}}$ in the spring

pool was caused by the dissolution of calcite or the degradation of soil organic matter for the following reasons. First, the degradation of soil organic matter would be the most intense during midday when the air temperature was the highest, resulting in more CO_2 entering the groundwater. This would affect the $\delta^{13}\text{C}_{\text{DIC}}$ in two ways. On the one hand, lighter CO_2 from soil organic matter degradation would cause depletion of the $\delta^{13}\text{C}_{\text{DIC}}$. On the other hand, higher CO_2 could drive calcite dissolution and increase the $\delta^{13}\text{C}_{\text{DIC}}$ because of the heavier $\delta^{13}\text{C}$ of limestone. Because the $\delta^{13}\text{C}_{\text{DIC}}$ at 13:30 was the highest, organic matter degradation is not likely the main influence on the $\delta^{13}\text{C}_{\text{DIC}}$. Second, the SiC , $[\text{Ca}^{2+}]$ and $[\text{HCO}_3^-]$ of the spring were stable and SiC was always slightly below 0 (Fig. 3), indicating the groundwater was undersaturated with respect to calcite. This suggests that there was little precipitation/dissolution of limestone in the spring. Because the diurnal variation of the $\delta^{13}\text{C}_{\text{DIC}}$ in the spring pool is not likely controlled by organic matter degradation or calcite dissolution, it is most likely controlled by the change in CO_2 efflux or aquatic photosynthetic uptake of CO_2 .

CO_2 outgassing (efflux) causes an enrichment of $\delta^{13}\text{C}_{\text{DIC}}$ in the residual DIC. One study documented shifts in $\delta^{13}\text{C}_{\text{DIC}}$ of up to 5‰ as a result of CO_2 outgassing at carbonate springs (Michaelis et al., 1985). According to Fig. 5a and Table 3, CO_2 efflux was the weakest at the midday sampling and most intense in the evening. If CO_2 efflux was the primary influence on $\delta^{13}\text{C}_{\text{DIC}}$, then $\delta^{13}\text{C}_{\text{DIC}}$ should be the lightest at midday and the heaviest in the evening, the opposite of what is observed. Therefore, the observed $\delta^{13}\text{C}_{\text{DIC}}$ pattern is most likely related to the change in aquatic photosynthetic uptake of CO_2 by the submerged plants in the spring pool, stronger during midday when insolation is high than in the early morning and evening.

It should be pointed out, however, that we do not have a full diurnal time series of $\delta^{13}\text{C}_{\text{DIC}}$ values, which limits our ability to interpret the rates of change of the isotopes and thus the causes of the changes (e.g., carbonate mineral precipitation or dissolution, CO_2 degassing, and organic carbon oxidation).

In addition, the reason why all the physical and chemical parameters of the spring did not fluctuate was because the WTW350i electrode was placed in the spring orifice, free from any photosynthesis activity and thus reflecting the characteristics of groundwater without any modification from the open surface. Because photosynthesis utilizing CO_2 was most intense at noon-time and in the evening, CO_2 outgassing was the weakest at this time, consistent with our data from the floating chamber.

5.2. Mechanisms for diurnal variations in physical, chemical and isotopic properties of the midstream pond

Physical and chemical parameters of surface water may be controlled by groundwater input, temperature changes, gas exchange between water and atmosphere, aquatic photosynthesis and respiration, and calcite precipitation and dissolution (Spiro and Pentecost, 1991). These are discussed below.

(1) Groundwater input

From the data in Fig. 3, little or no diurnal variations were observed in the physical–chemical parameters of the Maolan spring: groundwater parameters were stable and thus the diurnal changes in physical and chemical properties in the midstream pond were not caused by changes in the groundwater input.

(2) Temperature

Solubility of both O_2 and CO_2 are temperature-dependent with higher solubility when water temperature is low. In the midstream

Table 2
Measured CO₂ concentration in the floating chamber.

Location	Time	CO ₂ ppmv				
Spring pool	Morning (7:31–7:39)	540	555	574	588	602
	Midday (13:25–13:33)	382	390	395	407	416
	Evening (19:43–19:51)	566	611	630	615	660
Midstream	Morning (7:49–7:55)	517	560	552	544	
	Midday (14:51–14:59)	364	329	312	284	273
	Evening (20:13–20:21)	491	494	516	509	518
Downstream	Morning (8:09–8:17)	534	546	538	543	551
	Midday (15:17–15:25)	385	440	402	404	434
	Evening (20:48–20:56)	446	467	446	454	470

Table 3
Estimation of CO₂ flux (F) in the floating chamber in Maolan spring pool and the spring-fed two ponds in the morning, midday and evening.

Location	Time	F (mg/s/m ²)	F (mg/h/m ²)	F (mg/d/m ²)
Spring pool	Morning (7:31–7:39)	0.029	100	2500
	Midday (13:25–13:33)	0.016	57	1400
	Evening (19:43–19:51)	0.035	130	3100
Midstream pond	Morning (7:49–7:55)	0.013	47	1100
	Midday (14:51–14:59)	−0.042	−150	−3600
	Evening (20:13–20:21)	0.0123	46	1100
Downstream pond	Morning (8:09–8:17)	0.0058	21	500
	Midday (15:17–15:25)	0.011	40	960
	Evening (20:48–20:56)	0.0065	24	560

§ Flux(mg/s/m²) = 0.001963 * (dc/dt) * (V/A) * (273.15/T_m) * (P_m/101.325).

Flux(mg/h/m²) = 7.069 * (dc/dt) * (V/A) * (273.15/T_m) * (P_m/101.325).

Flux(mg/d/m²) = 169.6 * (dc/dt) * (V/A) * (273.15/T_m) * (P_m/101.325).

where dc/dt: change rate in CO₂ partial pressure in the floating chamber; V: chamber volume; A: chamber bottom area; 273.15: standard temperature in K; T_m: the measured temperature of the sampling day in K; P_m: the measured pressure on the sampling day in kPa; 101.325: standard pressure in kPa.

The “−” sign indicates CO₂ influx, and the positive values mean effluxes.

pond, pH and DO increased and pCO₂ decreased when water temperature increased during the day, and all trends reversed as temperature decreased at night (Fig. 6a and b). Although the pH and pCO₂ trends follow the expected trends for temperature control on gas solubility, the DO trend is the opposite of what is expected. Therefore, the changes in water temperature might not be the major factor controlling pH, pCO₂, and DO in the midstream pond during the study period.

(3) Gas exchange between water and atmosphere

Inland streams and rivers tend to be CO₂-supersaturated with respect to the atmosphere and thus, are a net source of CO₂ to the atmosphere (Butman and Raymond, 2011). Khadka et al. (2014) estimates that the pCO₂ of a karst river water could be as high as 105 times supersaturated with respect to the atmospheric CO₂. Gas exchange between water and air can induce large diurnal variations in DO and pCO₂, the major controls of Eh and pH (Hoffer-French and Herman, 1989; Liu et al., 2006, 2008). In this study, pCO₂ and DO followed opposite trends in the midstream pond (Fig. 6c).

CO₂ outgassing should be the weakest at midday and highest in the morning in the midstream pond, as inferred from the estimated pCO₂ values and measured CO₂ concentrations in the floating chamber (Fig. 5, Table 2). CO₂ degassing enriches δ¹³C_{DIC} in streams (Doctor et al., 2008). The expected highest rate of outgassing in the early morning should have yielded the highest δ¹³C_{DIC}. Instead, the highest δ¹³C_{DIC} was at midday, when the estimated pCO₂ was the lowest.

These observations and trends indicate that outgassing may not have been the dominant factor controlling pH, concentrations of DO and CO₂, and δ¹³C_{DIC} during the study period. Our observations

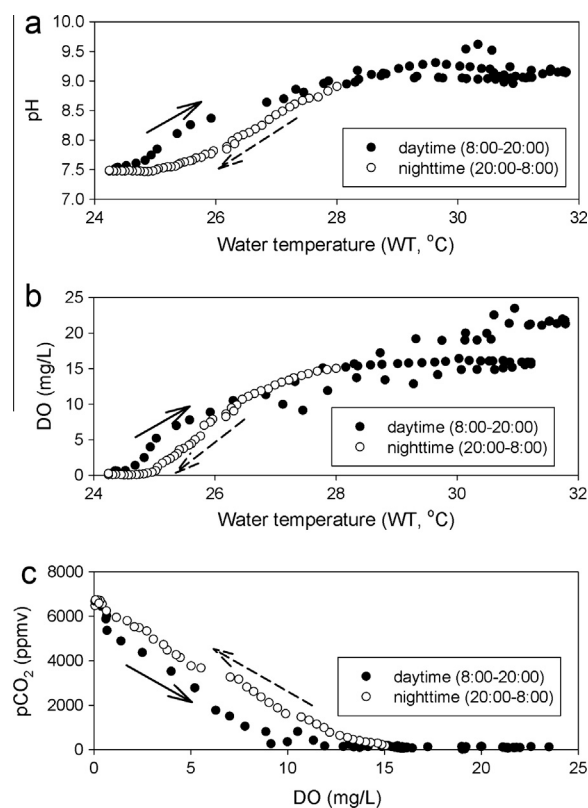
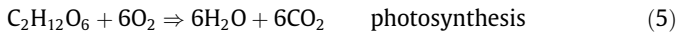


Fig. 6. Relationship between pH and water temperature (a), between DO and water temperature (b), and between pCO₂ and DO (c) in the midstream pond (2-sigma error bars are smaller than the symbols).

agree with Khadka et al. (2014) who state that CO₂ degassing does not fully control the δ¹³C enrichment in water.

(4) Photosynthesis and respiration by submerged plants

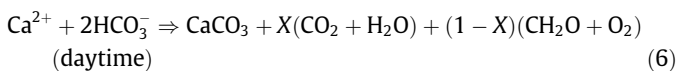
Diurnal variations of DO and pCO₂ are commonly influenced by aquatic photosynthesis and respiration processes which can be approximated by standard equations (e.g., Liu et al., 2008):



Measured DO showed positive variation with water temperature, and inverse correlation with pCO₂ (Fig. 6), suggesting a link to photosynthesis and respiration. During the day when the rate of photosynthesis exceeded respiration, submerged plants used DIC and the energy from the sunlight to produce organic matter and O₂. Fig. 3 shows that when sunlight was strong during the day, water temperature increased until 16:00 and DO increased until 18:00. pH of the water increased as photosynthesis consumed CO₂. On the other hand, respiration occurs at all times, consuming O₂ and releasing CO₂. Therefore, after 16:00 when water temperature started to decrease, DO and pH decreased by the respiration release of CO₂ into the water, with a time lag of one or two hours. During the night, in the absence of photosynthesis, respiration was dominant, and consequently DO and pH fell to their minima and pCO₂ peaked (Fig. 3). The inverse relationship between pCO₂ and DO over the study period (Fig. 6c) suggests that the effect of aquatic biological processes surpassed the temperature effect and out-gassing. We suggest biological processes are the main factors dominating pH, concentrations of DO and CO₂, and δ¹³C_{DIC} in the midstream pond on a daily timescale under climatic conditions similar to those during the study period.

(5) Calcite precipitation/dissolution

The decrease in Ca²⁺ concentration between Maolan spring and the midstream pond (Fig. 3, Table 1) suggests that calcite was being precipitated in the midstream pond. During the daytime, submerged plants utilize CO₂ and therefore DIC in the ponds, thereby increasing the pH, and potentially driving calcite precipitation. During the nighttime, with the absence of photosynthesis, submerged plants release CO₂ back into the water by respiration, thereby increasing the solubility of calcite, and potentially driving calcite dissolution in the midstream pond. The following equations can express these processes (Liu et al., 2011):



where X and 1–X are stoichiometric numbers.

When calcite precipitates (which enriches ¹³C in the carbonate, with ~2‰ heavier than HCO₃⁻, Deines et al., 1974) and organic matter forms (which depletes ¹³C in the pool, with ~15‰ lighter than HCO₃⁻, Sun et al., 2011) during the day, EC, Ca²⁺ and HCO₃⁻ concentrations all decrease, causing depletion of ¹²C in the remaining DIC in water (i.e., increase in δ¹³C_{DIC}). At night, the EC, Ca²⁺, HCO₃⁻ concentrations increase due to calcite dissolution and δ¹³C_{DIC} decreases due to release of light ¹²CO₂ into water from respiration. However, EC, Ca²⁺ and HCO₃⁻ in the midstream pond never exceeded those in Maolan spring (Fig. 3). Moreover, SIC of the midstream water ranged from 0.03 to 1.62 which is always at least slightly oversaturated with respect to calcite, indicating no carbonate dissolution. The SIC values in present study are compared with those from another study of a karst river by De Montety et al.

(2011), who showed that river water was slightly undersaturated relative to calcite (minimum SIC of –0.01) during the night and highly oversaturated during the day. Therefore, carbonate dissolution in the midstream pond is an unlikely mechanism contributing to variations in DIC concentrations and δ¹³C_{DIC} on a daily timescale.

5.3. Mechanisms for diurnal variations in physical, chemical and isotopic properties of the downstream pond

The same factors addressed in the midstream pond also apply to the downstream pond. When the sun rose at 8:00, the water temperature started to increase and DO increased rather than decreased. Thus, the DO increase likely resulted from aquatic photosynthesis. pCO₂ decreased causing higher pH. The variations of the chemical parameters in the downstream pond were much less than those in the midstream pond, as were variations in δ¹³C_{DIC} values. In the downstream pond, however, the δ¹³C_{DIC} value lower at midday than in the evening may be explained by the deposition of more calcite at midday, which is enriched in ¹³C, leaving DIC rich in ¹²C (Deines et al., 1974; Michaelis et al., 1985).

The reduced amplitude of the variations in the downstream pond in comparison with the midstream pond may result from the larger volume in the downstream pond that buffered the system. The depth of the downstream pond water was around 1 m, while the depth of the midstream pond water was less than 0.2 m. With the surface areas of about 1310 m² and 284 m², water volumes were estimated to be about 1300 m³ and 60 m³ in the downstream and midstream ponds, respectively. The volume effect was further intensified by the lower biomass (submerged plants) in the downstream pond than in the midstream pond, as indicated by the water color (Fig. 2).

5.4. Contribution of aquatic biological effects to the stability and sink of carbon

(1) Transformation of DIC into OC: organic carbon preservation potential

The initial DIC of the midstream pond water was contributed mainly by the Maolan spring and the initial DIC of the downstream pond water was controlled by the midstream pond water input. DIC concentration in the midstream and downstream ponds were always lower than that of the spring water. The average estimated DIC concentration of the spring was 224 mg/L, while the average estimated DIC concentrations of the midstream and downstream ponds were 187 mg/L and 182 mg/L, respectively. The decrease in the DIC concentrations between the spring and the midstream pond, and between the midstream pond and the downstream pond reflects the loss of inorganic carbon. The processes influencing the DIC concentrations in the two ponds were: (1) precipitation and dissolution of calcite, (2) exchanges with atmospheric CO₂, and (3) aquatic photosynthetic and respiratory.

Since this loss of DIC will be partly transformed into OC (Sun et al., 2011) as stated in Eq. (6), and eventually partly buried as autochthonous organic matter (OC(s)) (Liu et al., 2011, Fig. 7), it constitutes a “biological carbon pump” (De La Rocha and Passow, 2007) and increases the organic carbon preservation potential in the ponds. Moreover, if the terrestrial “biological carbon pump” effect is strong enough, as in the case of midstream pond, there is even a CO₂ sink directly from the atmosphere to surface waters (Fig. 5b, Table 3) as discussed below in more detail.

(2) CO₂ influx from atmosphere to water: insight from the floating chamber data in the midstream pond

During 13:00–19:00, the strong aquatic photosynthesis (with high DO concentrations) resulted in pCO₂ levels of less than

Table 4
Comparison of CO₂ degassing to the atmosphere from some carbonate-dominated rivers in the world.

River/region	Climate	Average CO ₂ degassing rate (t C/km ² /a)	References
Changjiang river	Subtropic	186–410	Zai et al. (2007)
Xijiang river	Humid subtropic	830–1560	Yao et al. (2007)
Santa Fe river	Subtropic	402–1156	Khadka et al. (2014)
Maolan spring-ponds	Subtropic	–139 to 232	This study

100 ppmv (Fig. 3, Table 1). Further, CO₂ concentration in the chamber started with 364 ppmv at 14:51 then gradually decreased to 273 ppmv after 8 min (Fig. 5b). The pCO₂ in the chamber was lower than that of the atmosphere (around 390 ppmv), suggesting that there was CO₂ influx from the atmosphere to water instead of CO₂ evasion. This phenomenon in the midstream pond suggests that strong aquatic photosynthesis in terrestrial surface waters might form another important natural carbon sink by drawing CO₂ directly from the atmosphere, as occurs in the oceans (Ducklow et al., 2001; Passow and Carlson, 2012). Due to the strong biological pump effect, the average CO₂ degassing flux for Maolan Karst spring-ponds is much less compared with the other karst rivers in the world (Table 4), where underwater photosynthesis may be weak (evidenced by low DO values, generally <8 mg/l). When the biological pump effect was strong enough, there was even an influx from air to water, showing the importance of underwater photosynthesis in both stabilizing the carbon sink (as DIC) by carbonate dissolution (Table 4) and creating new carbon sink directly from atmosphere.

(3) Quantification of daily organic carbon formation in the two ponds

The decrease in DIC between Maolan spring and the ponds results from the joint effects of calcite precipitation, exchanges with atmospheric CO₂, and aquatic photosynthesis. We have used the decrease in Ca²⁺ concentrations to predict calcite precipitation (Table 1) and the flux of exchanges with atmospheric CO₂ (Table 3) in the two ponds. The daily organic carbon formation in the two ponds can be estimated as follows:

$$M_{OC} = Q * (DIC_1 - DIC_2)/5.080 - Q * (Ca_1 - Ca_2)/3.337 - (F/3.664) * A$$

where M_{OC} is mass of organic carbon formed in a day (mg/d); Q is the discharge of the stream (i.e., the discharge of the spring if evaporation is ignored under conditions of high humidity, L/d), DIC₁ and DIC₂ are the HCO₃⁻ concentrations at the inlet and outlet of the pond (in mg/L), 5.080 is the HCO₃⁻–carbon conversion factor, Ca₁ and Ca₂ are the Ca²⁺ concentrations in mg/L at the inlet and outlet of the pond, respectively, 3.337 is the calcium–carbon conversion factor, (40.08/12.011), F is the CO₂ flux from water surface (mg/d/m²), 3.664 is the CO₂–carbon conversion factor, and A is the area of pond water surface (m²).

For the midstream pond:

$$M_{OC} = 103680 * (223.6 - 186.6)/5.080 - 103680 * (53.5 - 44.8)/3.337 - (-450/3.664) * 280 = 519000 \text{ (mg/d)}$$

For the downstream pond:

$$M_{OC} = 103680 * (186.6 - 182)/5.080 - 103680 * (44.8 - 43.7)/3.337 - (670/3.664) * 1300 = -178000 \text{ (mg/d)}$$

Therefore, the organic carbon sink flux by the submerged plants in the midstream pond is ~1850 mg/d/m², equivalent to 677 t C/km²/a, which shows the significant role of submerged plants in stabilizing the carbon sink by karst processes (carbonate weathering) (from DIC to OC) and/or uptake of CO₂ directly from the atmosphere.

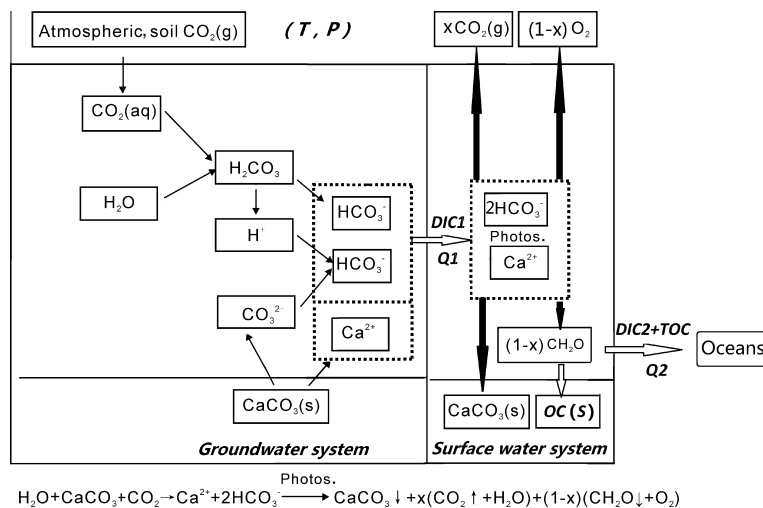


Fig. 7. Conceptual model of the carbon cycle in karst settings based on water-rock-gas-biota interactions (drawing in reference to Liu et al. (2011)). T, P and Q are the air temperature, precipitation and discharge of a karst catchment area respectively. DIC₁ and DIC₂ are the concentrations of dissolved inorganic carbon in the karst underground water system and surface water system respectively, and TOC is the concentration of total organic carbon in surface water system transformed from DIC₁ by the submerged plants via photosynthesis. OC(s) is the sedimentation of organic carbon. Note: Unlike the traditional carbonate weathering carbon cycle model, which only considers water-rock-gas interaction (ignoring the organic matter deposition formed by aquatic photosynthetic uptake of DIC), this model helps to answer important questions such as whether carbonate weathering could be a long-term carbon sink, if accompanied by burial of autochthonous organic matter, thus controlling long-term climate change.

The organic carbon sink flux in the downstream pond is -137 mg/d/m^2 , equivalent to $-49.9 \text{ t C/km}^2/\text{a}$, the negative value showing no net organic carbon sink by the few submerged plants in the downstream pond, but, instead, release of CO_2 by decomposition of allochthonous organic matter. We assume this organic matter is the legacy of fish farming, ceased ~ 1 year before this study, in the downstream pond.

6. Conclusions

Physical and chemical parameters (water temperature, pH, DO, and EC) were monitored at high time-resolution (15 min) over a 30-hour period to investigate the controls on hydrobiogeochemistry at the Maolan Karst Experimental Site, Guizhou province, China. The study site included a karst spring and two downstream ponds with different development of submerged plants, and sampling occurred under summer, sunny, base-flow conditions, when underwater photosynthesis was strongest. $[\text{Ca}^{2+}]$, $[\text{HCO}_3^-]$, CO_2 partial pressure ($p\text{CO}_2$) and saturation index of calcite (SIc) were estimated from the high-resolution measurements. Samples for $\delta^{13}\text{C}_{\text{DIC}}$ were collected three times over the 30-hour period (midday, early evening and early morning) at the three locations. Gas samples collected from a floating chamber were used to calculate CO_2 efflux from the three locations.

Results show that there was little or no diurnal variation in most of the spring physical and chemical parameters. The midstream pond, assumed to have received input only from the spring $\sim 38 \text{ m}$ upgradient, was filled with submerged plants, and all physical and chemical parameters showed distinct diurnal changes. The temperature, pH, DO, SIc, $\delta^{13}\text{C}_{\text{DIC}}$ in the midstream pond increased during the day and decreased at night, while EC, HCO_3^- , Ca^{2+} , and $p\text{CO}_2$ decreased during the day and increased at the night. The maximum DO values ($16\text{--}23 \text{ mg/L}$) in the midstream pond during the day were twice to three times those expected of water equilibrated with atmospheric O_2 , and suggesting strong aquatic photosynthesis. The midstream pond had the lowest estimated $p\text{CO}_2$ of the three locations, at 20 ppmv, which is much less than the atmospheric CO_2 concentration, also suggesting aquatic photosynthesis. In addition, during the midday sampling time, the CO_2 flux direction was from the atmosphere into water. The downstream pond had only a few submerged plants. At this location, all of the parameters varied similarly to the midstream pond, but with much lower amplitude. We suggest that this results from the dilution effect because of the lower biomass/water tank ratio. The diurnal hydrobiogeochemical temporal variations in the two ponds are consistent with results expected from aquatic photosynthesis and respiration.

The large loss of DIC between spring and midstream pond is attributed to biological storage of carbon, demonstrating that natural surface waters may constitute an important carbon sink. Since this loss of DIC is at least partly and likely mostly transformed into OC, burial as autochthonous organic matter constitutes a “terrestrial biogeochemical carbon pump” (TBCP). Moreover, if the TBCP effect is strong enough, as in the case of midstream pond under optimum photosynthesis conditions, there is a CO_2 sink directly from the atmosphere to surface waters.

The distribution and extent of surface waters with strong TBCP is as yet unknown. In addition, sedimentation and preservation rates of autochthonous OC (Fig. 7) in terrestrial surface water is also poorly known, especially under rapid global climate and land use changes occurring recently. However, with the changing climate and the ecological systems, the link between dissolution and precipitation within the carbonate areas may be altered, leading to a net influence on the local or global carbon cycle (Martin et al., 2013). This study suggests that an important goal in improv-

ing global carbon budgets may include quantifying the importance of the TBCP in terrestrial aquatic settings.

Acknowledgments

This work was supported by the 973 Program of China (2013CB956703), the KU Department of Geology Research Grant, the National Natural Science Foundation of China (41172232 and 41430753), and the open fund of the State Key Laboratory of Environmental Geochemistry. Special thanks are given to Derek Ford for his thoughtful comments and suggestions, which greatly improved the original draft.

References

- Aucour, A.M., Sheppard, S.M.F., Guyomar, O., Wattalet, J., 1999. Use of ^{13}C to trace origin and cycling of inorganic carbon in the Rhone river system. *Chem. Geol.* 159, 87–105.
- Butman, D., Raymond, P.A., 2011. Significant efflux of carbon dioxide from streams and rivers in the United States. *Nat. Geosci.* 4, 839–842.
- Cerling, T.E., Solomon, D.K., Quade, J., 1991. On the isotopic composition of carbon in soil carbon dioxide. *Geochim. Cosmochim. Acta* 55, 3403–3405.
- De La Rocha, C.L., Passow, U., 2007. Factors influencing the sinking of POC and the efficiency of the biological carbon pump. *Deep Sea Res.* 54, 639–658.
- De Montety, V., Martin, J.B., Cohen, M.J., Foster, C., Kurz, M.J., 2011. Influence of diel biogeochemical cycles on carbonate equilibrium in a karst river. *Chem. Geol.* 283, 31–43.
- Deines, P., Langmuir, D., Harmon, R.S., 1974. Stable carbon isotope ratios and the existence of a gas phase in the evolution of carbonate ground waters. *Geochim. Cosmochim. Acta* 38, 1147–1164.
- Doctor, D.H., Kendall, C., Sebestyen, S.D., Shanley, J.B., Ohte, N., Boyer, E.W., 2008. Carbon isotope fractionation of dissolved inorganic carbon (DIC) due to outgassing of carbon dioxide from a headwater stream. *Hydrol. Proc.* 22, 2410–2423.
- Ducklow, H.W., Steinberg, D.K., Buesseler, K.O., 2001. Upper ocean carbon export and the biological pump. *Oceanography* 14, 50–58.
- Han, G., Tang, Y., Wu, Q., 2010. Hydrogeochemistry and dissolved inorganic carbon isotopic composition on karst groundwater in Maolan, southwest China. *Environ. Earth Sci.* 60, 893–899.
- Hayashi, M., Vogt, T., Machler, L., Schirmer, M., 2012. Diurnal fluctuations of electrical conductivity in a pre-alpine river: effects of photosynthesis and groundwater exchange. *J. Hydrol.* 450, 93–104.
- Hoffer-French, K., Herman, J., 1989. Evaluation of hydrological and biological influences on CO_2 fluxes from a karst stream. *J. Hydrol.* 108, 189–212.
- Jiang, G., Guo, F., Wu, J., Li, H., Sun, H., 2008. The threshold value of epikarst runoff in forest karst mountain area. *Environ. Geol.* 55, 87–93.
- Khadka, M., Martin, J., Jin, J., 2014. Transport of dissolved carbon and CO_2 degassing from a river system in a mixed silicate and carbonate catchment. *J. Hydrol.* 513, 391–402.
- Kurz, M.J., de Montety, V., Martin, J.B., Cohen, M.J., Foster, C.R., 2013. Controls on diel metal cycles in a biologically productive carbonate-dominated river. *Chem. Geol.* 358, 61–74.
- Liu, Z., Groves, C., Yuan, D., Meiman, J., Jiang, G., He, S., 2004. Hydrochemical variations during flood pulses in the southwest China peak cluster karst: Impacts of $\text{CaCO}_3\text{--H}_2\text{O--CO}_2$ interactions. *Hydrol. Proc.* 18, 2423–2437.
- Liu, Z., Li, Q., Sun, H., Liao, C., Li, H., Wang, J., Wu, K., 2006. Diurnal variations of hydrochemistry in a travertine-depositing stream at Baishuitai, Yunnan, SW China. *Aquat. Geochem.* 12, 103–121.
- Liu, Z., Li, Q., Sun, H., Wang, J., 2007. Seasonal, diurnal and storm-scale hydrochemical variations of typical epikarst spring in subtropical karst areas of SW China: soil CO_2 and dilution effects. *J. Hydrol.* 337, 207–223.
- Liu, Z., Liu, X., Liao, C., 2008. Daytime deposition and nighttime dissolution of calcium carbonate controlled by submerged plants in a karst spring-fed pool: insights from high time-resolution monitoring of physico-chemistry of water. *Environ. Geol.* 55, 159–1168.
- Liu, Z., Dreybrodt, W., Wang, H., 2010. A new direction in effective accounting for the atmospheric CO_2 budget: Considering the combined action of carbonate dissolution, the global water cycle and photosynthetic uptake of DIC by aquatic organisms. *Earth-Sci Rev.* 99, 162–172.
- Liu, Z., Dreybrodt, W., Liu, H., 2011. Atmospheric CO_2 sink: silicate weathering or carbonate weathering? *Appl. Geochem.* 26, 292–294.
- Martin, J., Brown, A., Ezell, J., 2013. Do carbonate karst terrains affect the global carbon cycle? *Acta Carsol.* 42, 187–196.
- Michaelis, J., Uzdowski, E., Menschel, G., 1985. Partitioning of ^{13}C and ^{12}C on the degassing of CO_2 and the precipitation of calcite—Rayleigh type fractionation and a kinetic model. *Am. J. Sci.* 285, 318–327.
- Parkhurst, D.L., Appelo, C.A.J., 1999. User's guide to PHREEQC (Version 2)—a computer program for speciation, batch-reaction, one-dimensional transport, and inverse geochemical calculations. US Geol. Surv. Wat-Resour. Invest. Rep. 99–4259, 312.

- Passow, U., Carlson, C.A., 2012. The biological pump in a high CO₂ world. *Mar. Ecol. Prog. Ser.* 470, 249–271.
- Spiro, B., Pentecost, A., 1991. One day in the life of a stream—a diurnal inorganic carbon mass balance for a travertine-depositing stream (Waterfall Beck, Yorkshire). *Geomicrobiol. J.* 9, 1–11.
- Sun, H., Han, J., Zhang, S., Lu, X., 2011. Transformation of dissolved inorganic carbon (DIC) into particulate organic carbon (POC) in the lower Xijiang River, SE China: an isotopic approach. *Biogeosci. Discuss.* 8, 9471–9501.
- Telmer, K., Veizer, J., 1999. Carbon fluxes, pCO₂ and substrate weathering in a large northern river basin, Canada: carbon isotope perspectives. *Chem. Geol.* 159, 61–86.
- Yang, R., Liu, Z., Zeng, C., Zhao, M., 2012. Response of epikarst hydrochemical changes to soil CO₂ and weather conditions at Chenqi, Puding, SW China. *J. Hydrol.* 468–469, 151–158.
- Yao, G., Gao, Q., Wang, Z., Huang, X., He, T., Zhang, Y., Jiao, S., Ding, J., 2007. Dynamics of CO₂ partial pressure and CO₂ outgassing in the lower reaches of the Xijiang River, a subtropical monsoon river in China. *Sci. Total Environ.* 376, 255–266.
- Zai, W., Dai, M., Guo, X., 2007. Carbonate system and CO₂ degassing fluxes in the inner estuary of Changjiang (Yangtze) River, China. *Mar. Chem.* 107, 342–356.
- Zeng, C., Gremaud, V., Zeng, H., Liu, Z., Goldscheider, N., 2012. Temperature-driven meltwater production and hydrochemical variations at a glaciated alpine karst aquifer: implication for the atmospheric CO₂ sink under global warming. *Environ. Earth Sci.* 65, 2285–2297.
- Zhou, Z., 1987. *Scientific Survey of the Maolan Karst Forest*. Guizhou Peoples' Publishing House, Guiyang.